Integrated AWG Spectrometer for On-chip Optical Coherence Tomography and Raman Spectroscopy

B.I. Akca, N. Ismail, F. Sun, A. Driessen, K. Wörhoff, M. Pollnau, and R.M. de Ridder
Integrated Optical Microsystems Group,
MESA+ Institute for Nanotechnology, University of Twente
Enschede, The Netherlands
B.I.Akca@utwente.nl

V.Duc Nguyen, J. Kalkman, and T.G. van Leeuwen
Biomedical Engineering & Physics
Academic Medical Center,
University of Amsterdam
Amsterdam, The Netherlands

Abstract—**Silicon oxynitride-based arrayed waveguide grating (AWG) spectrometers were designed for on-chip spectral-domain optical coherence tomography (OCT) systems and Raman spectroscopy of the skin. A novel geometrical layout for Raman spectroscopy was introduced to reduce loss. Measurements show that integrated optics has a good potential for miniaturizing current OCT systems.**

Keywords-arrayed waveguide grating; Raman spectroscopy; optical coherence tomography; integrated optics

I. INTRODUCTION

Spectrometers have an important role in a wide variety of fields. The most important integrated optical implementation of a spectrometer is the AWG that, with its excellent performance and compactness, has a high potential for various spectroscopic applications [1]. Two of these applications are considered here: on-chip spectral-domain OCT systems and confocal Raman spectroscopy of the skin.

The operation of an AWG [1] is briefly explained, referring to Fig. 1a. Light from an input waveguide diverges in a first free propagation region (FPR) in order to illuminate the input facets of an array of waveguides with a linearly increasing length. At a central design wavelength, the phase difference at the output facets of adjacent array waveguides is an integer multiple of 2π. Since these facets are arranged on a circle, a cylindrical wavefront is formed at the beginning of a second FPR, which generates a focal spot at the central output channel. Since the phase shift, caused by the length differences between arrayed waveguides, is linearly dependent on wavelength, the resulting wavelength-dependent phase gradient implies a tilt of the cylindrical wavefront at the beginning of the second FPR, which causes the focal spot to shift to a different output waveguide.

II. AWG SPECTROMETER FOR ON-CHIP OCT SYSTEMS

OCT is a widely used optical imaging technology which can provide non-invasive, sub-micrometer resolution diagnostic images [2]. We aimed for a miniaturized OCT system operating at 1.3 μm, a commonly used wavelength for skin imaging. In the literature there is only limited data on the implementation of OCT systems on a chip [3-4].

The free spectral range (FSR) and wavelength resolution ($\Delta\lambda$) of the AWG were determined according to the depth resolution and depth range requirements of the OCT system. For the first device, we aimed at a 19-μm depth resolution (determined by the free spectral range of the AWG) and 1-mm depth range (determined by the wavelength spacing per output waveguide). Using the standard AWG equations [1], the remaining design parameters were determined as: optical path length difference 29.176 μm; grating order 33; focal length of the slab region 5393.5 μm; number of arrayed waveguides 400; and number of output waveguides 100. We used single-mode silicon oxynitride (SiON) channel waveguides with 2 μm width and 0.6 μm height, embedded in SiO_2. The core and cladding refractive indices were 1.55 and 1.4485, respectively, at 1.3 μm. The minimum bending radius of curved waveguides was calculated to be 800 μm. In order to decrease the loss, 6-μm-wide and 200-μm-long linear tapers were applied at the interfaces between slab and arrayed waveguides. The device geometry was optimized for minimum loss and an adjacent crosstalk of -10 dB using beam propagation (BPM) simulations. The simulation result of the final design is given in Fig. 1b.

The optical transmission measurements were performed by coupling TE-polarized light from a broadband source (Fianium SC450) into the input waveguide, using a single-mode polarization-maintaining fiber. The output signal was sent to an optical spectrum analyzer (iHR 550, Horiba Jobin Yvon) through a single-mode fiber. The transmission spectra measured at the output channels were normalized with respect to the transmission of a straight channel waveguide. The transmission spectra of four central channels are given in Fig. 1c. The inset of Fig. 1c represents the complete set of 100 transmission spectra of the device. As predicted, each channel works as a bandpass wavelength filter. The resolution of the device was $\Delta\lambda$ = 0.38 nm and the FSR was 38.8 nm, which are both very close to the design values of 0.4 nm and 40 nm, respectively. The measured 3 dB bandwidth of the output channels was about 0.3 nm and the channel crosstalk was approximately –32 dB. The insertion loss was measured as –1.5 dB for the central and –6.5 dB for the outer channels, respectively. For TM polarization, we obtained a slight shift of 1.36 nm for the central wavelength, which corresponds to an effective refractive index difference of $\sim 1.54\times10^{-3}$ between the two polarizations due to the waveguide birefringence.

This work is supported by the Dutch Smartmix-Memphis and Dutch IOP Photonic Devices

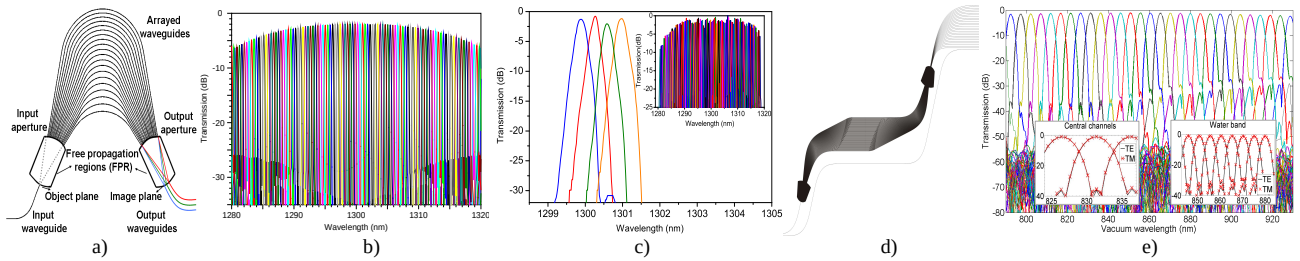

Figure 1. a) Schematic layout of an AWG. b) Beam propagation simulation result of the designed AWG. c) Optical transmission measurement results for the central output channels for TE polarization. The inset shows the complete free spectral range transmission data. d) AWG layout using identical bends (see text). e) Simulated wavelength response of the AWG for the skin application; the insets show the very low TE-TM shift.

III. AWG RAMAN SPECTROMETER

In vivo confocal Raman spectroscopy provides a possibility of accurately controlling the skin region from which the Raman signal is detected [5]. Here, we design an integrated, compact, and potentially low-cost device, specifically for the detection of water concentration in the *stratum corneum*. To this end, it is needed to measure the ratios between a broad water peak and narrow lipid and protein peaks in the Raman spectrum.

Our design is based on using SiON channel waveguides with SiO_2 cladding, having a cross-section of 1.4 µm × 0.52 µm. The core refractive index is 1.509 at 830 nm. At an excitation wavelength of 671 nm, the relevant Raman spectrum extends from 800 to 920 nm. In order to separate the lipid and protein peaks the output channel spacing is chosen as 5 nm, and to guarantee the lowest insertion loss for the lipid peak, the central wavelength of AWG is chosen at the center of the lipid band (831 nm). To cover the entire Raman signal a minimum free spectral range of 120 nm is required; the best choice of grating order is 3, resulting in 55 output channels. With our choice of channel spacing we can place only one channel in each of the L and P bands, and several channels are available for collecting the water and background signals.

The Raman signal may be up to 10^8 times weaker than the backscattered laser and fluorescence light; hence we introduce improvements in the geometrical layout of the device in order to reduce the losses. The standard anti-symmetric broadband layout [6] is modified in order to reduce the main sources of loss, which are intrinsically part of the conventional geometry. We identify these in straight-to-bend waveguide transition losses [7] and systematic phase errors due to the use of different bends for the arrayed waveguides. A method for reducing the systematic phase errors has been reported in [8], in which bends with constant bending radius (but different length) were used in all the arrayed waveguides. In our design we aimed to completely eliminate these phase errors by using identical bends in all arrayed waveguides. We use two bend types (A and B) as building blocks in all the arrayed waveguides. All arrayed waveguides are composed of two bends of type A and N-1 bends of type B, where N is the number of arrayed waveguides. In this way the phase of light propagating in each array waveguide is affected in the same way by the bends, while the optical path length difference is introduced only by straight sections. Since this approach is independent of the specific bend geometry, we could easily replace all circular bends with cosine bends in which the transition from straight to bend is gradual and can be designed to be adiabatic. In a conventional design, such a replacement would lead to an excessive calculation burden. The layout is shown in Fig. 1d and the BPM simulation results are given in Fig. 1e. We observed negligible TE-TM shifts of 0.01 nm for the central channels and 0.03 nm in the water band, see inset in Fig. 1d.

IV. CONCLUSIONS

SiON-based AWG spectrometers have been designed and fabricated for on-chip spectral-domain OCT systems and confocal Raman spectroscopy of the skin. The device for Raman spectroscopy presents improvements in the geometrical layout aimed at reducing losses and is designed to be polarization insensitive. Its optical characterization is currently under way. The device for on-chip OCT systems has been optically characterized and the measurement results are in good agreement with the simulation results. The spectrometer shows very good performance in terms of insertion loss, crosstalk, FSR, and resolution. The OCT depth resolution and the depth range were calculated as 19.2 µm and 1.1 mm, respectively, using the measurement results. In future work, we will include light delivery and collection waveguide channels as well as detector arrays connected to the AWG output channels.

V. REFERENCES

[1] M. K. Smit and C. van Dam, "PHASAR-based WDM-devices: principles, design and applications," IEEE J. Select. Topics Quantum Electron., vol. 2, pp. 236–250, 1996.

[2] D. Huang et al., "Optical coherence tomography," Science, vol. 254, pp. 1178-1181, 1991.

[3] D. Culemann, A. Knuettel, and E. Voges, "Integrated optical sensor in glass for optical coherence tomography", IEEE J. Select. Topics Quantum Electron. vol. 5, pp. 730-734, 2000.

[4] G. Yurtsever and R. Baets, "Towards integrated optical coherence tomography system on silicon on insulator", Proc. 2008 Symp. IEEE/ LEOS Benelux Chapter, Enschede, The Netherlands, pp.163-166, 2008.

[5] P. J. Caspers, G. W. Lucassen, R. Wolthuis, H. A. Bruining, and G. J. Puppels, "In vitro and in vivo Raman spectroscopy of human skin," Biospectroscopy, vol. 4, pp. S31-S39, 1998.

[6] R. Adar, C. H. Henry, C. Dragone, R. C. Kistler, and M. A. Milbrodt, "Broad-band array multiplexers made with silica waveguides on silicon," J. Lightwave Technol., vol. 11, pp. 212-219, 1993.

[7] M. K. Smit, "Progress in AWG design and technology," IEEE/ LEOS Workshop Fibers & Optical Passive Compon., pp. 26-31, 2005.

[8] F. M. Soares et al., "InP-based arrayed-waveguide grating with a channel spacing of 10 GHz," National Fiber Optic Engineers Conference (Optical Society of America, Washington DC), paper JThA239, 2008.